International Journal of Application or Innovation in Engineering & Management (IJAIEM)
Web Site: www.ijaiem.org Email: editor@ijaiem.org
Volume 5, Issue 4, April 2016 **ISSN 2319 - 4847**

Design and Analysis of Dual Mass Flywheel Based on The Principle of Compensation and Continuously Variable Stiffness

Mr. Lamkane A.A[1]. Prof. Kulkarni S.N.[2], Mr. Mali V.V.[3]

[1]. M.E. (Mechanical)(Design), V.V.P.Institute of Engineering & Technology, Solapur.

[2]. Professor and Vice Principal, V.V.P.Institute of Engineering & Technology, Solapur.

[3]. M.E. (Mechanical)(Design), V.V.P.Institute of Engineering & Technology, Solapur.

ABSTRACT

The new dual mass flywheel structure (DMF) with continuously variable stiffness based on the principle of compensation offered to release the impact of the changes produced by progressive rigidity. Theoretical calculations and experiments, the structure and design of the proposal is found to be in theory possible to reduce torsional vibrations in machines with high power and high engine power transmission system TORQUE. Natural characteristics of the DMF machine transmission system torsional stiffness are analyzed to investigate the effect of first-class and second-class speed you. The results show that the new DMF, can reduce a large twist angle of the engine idle speed to achieve high couples , and avoid the effects of sudden changes in stiffness . Balance inertia compensation device , which runs the successful practice of engineering theory can apply to each part of the proposal process produces torque compensation is to eliminate disabling force .

Key Words - Dual mass flywheel, torsional vibration, inertia forces.

1. Introduction

The clutch system in a vehicle performs two main functions:

- Power interruption and modulation during start up and when shifting
- Reduction of rotational vibrations in the drive train induced by engine irregularities During the LuK Clutch Symposium, LuK will introduce some new developments which successfully fulfill these functions for our customers. The following presentation will illustrate a cross-section of development efforts aimed at reducing engine-induced rotational vibrations in the drive train. Rotational vibrations affect durability of the drive train components and create
- Gear rattle
- Body boom
- Tip-in/back-out vibrations

These factors produce considerable noise and a loss in driving comfort. The main cause of these rotational vibrations is variation in torque. This variation results from the discrete piston combustion cycle of the engine as a function of the ignition frequency. The vehicle drive train is a vibrating system. Figure 1 shows a simple model designed to simulate fundamental vibration behavior. The engine, transmission and vehicle are represented as rotating inertias connected by springs. The spring C3 represents the stiffness of the drive train, while spring C2, located between engine and transmission, represents the spring characteristic of the torsion damper. Such a system has two vibrations modes. The first mode, with a natural frequency of between 2 and 10 Hz, is known as the tip-in/back-out reaction. This is generally excited by a driver-induced load change. The second mode, where the transmission inertia vibrates against engine and vehicle, has a natural frequency of 40 - 80 Hz with conventional torsion dampers. This is a typical cause of

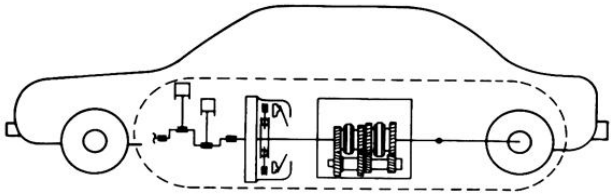

gear rattle.

mode 1

surging

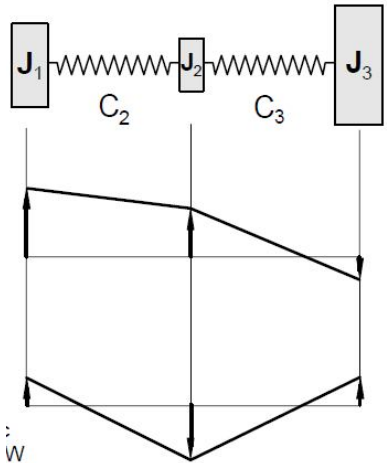

Fig. 1: Vehicle drive train with vibration

f = 2 - 10 Hz Engine transmission vehicle

mode 2

noise

f = 40 - 80 Hz clutch disc

f = 7,5 - 15 Hz DFC/DMFW

Consequently, the tuning of a conventional automotive torsion damper – a clutch disc with its corresponding spring characteristic - always involves compromise. The upper graph of Figure 2 shows typical speed fluctuations in a vehicle with a clutch disc. In this case, the friction-damped resonance is located at around 1700 rpm. Further damping of this resonance leads to a worsening of the hypercritical isolation of rotational vibrations (at speeds higher than the resonance).

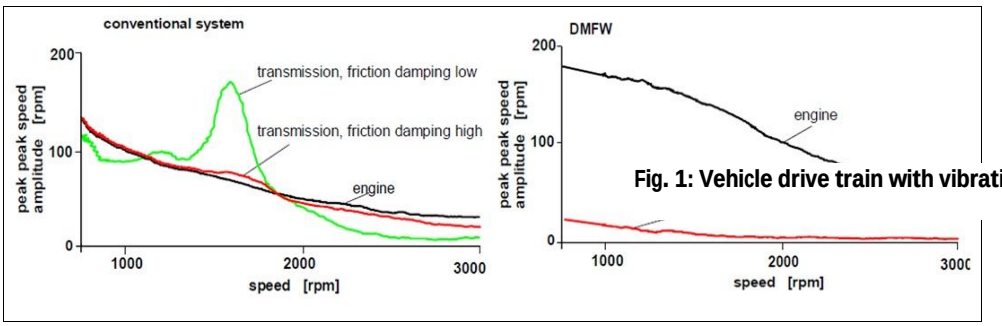

Figure 2: Torsional vibration isolation with conventional clutch disc and dual mass flywheel

1.1 Advantages of the DMFW

Although not everyone wants the DMFW due to the costs, the achievable improvements are so clear that it is being used extensively in large vehicles. The most important advantages will be outlined below.

1.1.1 Isolation from Torsional Vibrations

The primary feature of the DMFW is the almost complete isolation of torsional vibrations. This has been discussed extensively in earlier presentations and will only be summarized here. Figure 4 illustrates the angle accelerations at the transmission input for a conventional system with a torsion damper in the clutch disc (left) in comparison to a DMFW (right). With the torsion damper in the clutch disc, there is no significant vibration isolation achieved at low speeds. Resonance can be avoided by selecting appropriate damping.

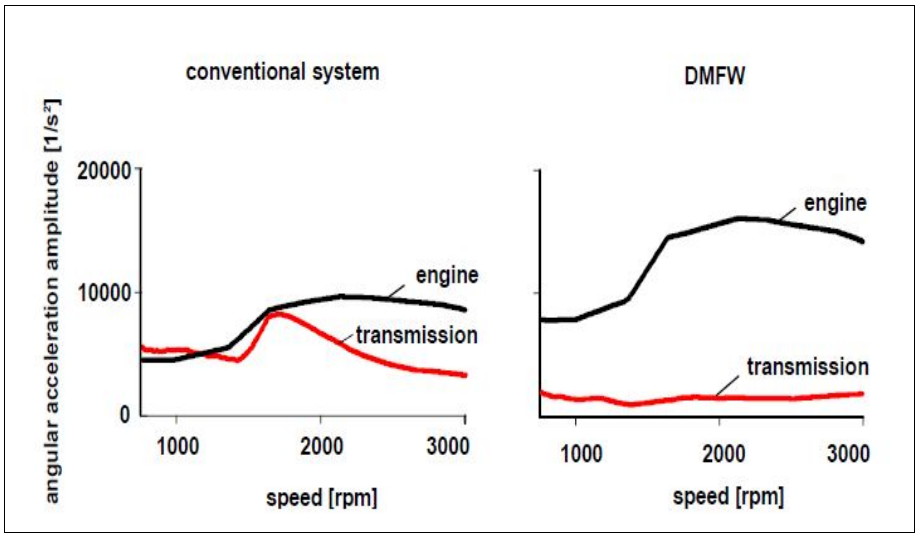

Figure 3: Comparison of vibration isolation of a conventional system to a dual mass flywheel

In contrast, the DMFW almost completely filters out the engine irregularity. Resonance generally no longer occurs in the driving range. Gear rattle no longer occurs due to the almost uniform operation of the secondary flywheel side and thus also of the transmission input shaft. Annoying droning can also be almost completely eliminated. The irregularity of the engine itself becomes greater with DMFW because the primary flywheel mass is lower than the conventional flywheel mass with a clutch. Therefore, the accessory drive must occasionally be returned. The smaller primary flywheel mass also has advantages, as will be presented later. Good vibration isolation, particularly during low-speed driving, often leads to low-consumption operation, which saves fuel due to the predominantly low engine speeds used. Many modern engines with a relatively flat torque curve favor this consumption-reducing operation.

2. Structure of the DMF based on compensation principle

Fig. 1 shows the structure of DMF based on the compensation principle, which is mainly made up of primary flywheel, shock absorber, drive plate, secondary flywheel, compensation device, inertia balance mechanism, bearing inner ring, pressure plate and end cover. The shock absorber (including springs and spring seats) is arranged in the intracavity of the primary flywheel, and the drive plate is fixed on the secondary flywheel by bolts. The compensation device and inertia balance mechanism are mounted on the secondary flywheel, and the bearing inner ring and three bearing block are put into the intracavity of the secondary flywheel and sealed by the pressure plate. In addition, the connection of bearing inner ring and end cover by bolts forms a journal bearing, which is finally fixed with the primary flywheel. Fig. 4 presents the change in stiffness of DMF. Fig. 4a is the initial state. In the DMF's operation, the secondary flywheel is assumed to rotate relative to the primary flywheel. Spring seat 1 rotates due to the action of the drive plate fixed on the secondary flywheel. While there are no contacts among all the spring seats shown in Fig. 4b, in which case springs 1, 2 and 3 installed between these spring seats are connected in series, and thus the first-stage stiffness of the DMF is formed. On the other hand, after turning a certain angle, spring seat 3 makes contact with spring seat 4, in which case, spring 3 is no longer pressed while springs 1 and 2 are in series and continue to be compressed. Thus the second-stage stiffness is generated, as shown in Fig. 4c. Besides, when

spring seat 2 is in connection with spring seat 3 (already contact with spring seat 4), only spring 1 with the largest stiffness can continue to be pressed until spring seat 1 contacts with spring seat 2 (i.e., the torsional angle reaches the maximum value), and thus, the third-stage stiffness comes into being, as shown in Fig. 4d.

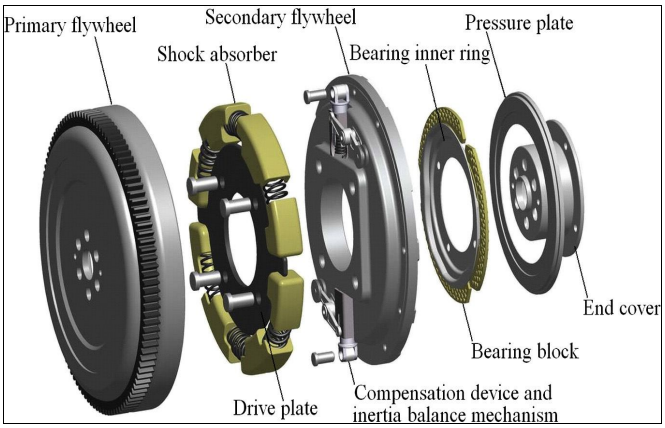

Fig 4: Structure of DMF based on compensation principle

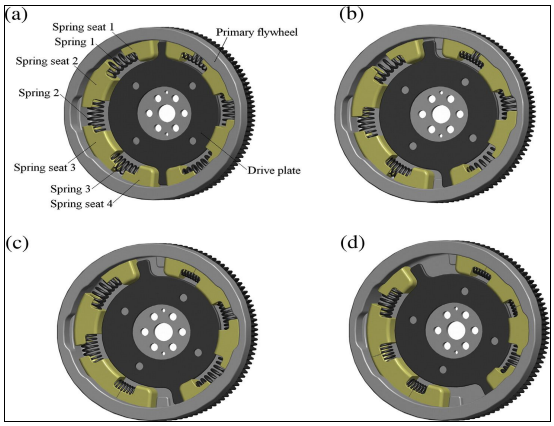

Fig 5: Chang in stiffness of DMF: (a) initial state; (b) the first-stage stiffness; (c) the second-stage stiffness; (d) the third-stage stiffness

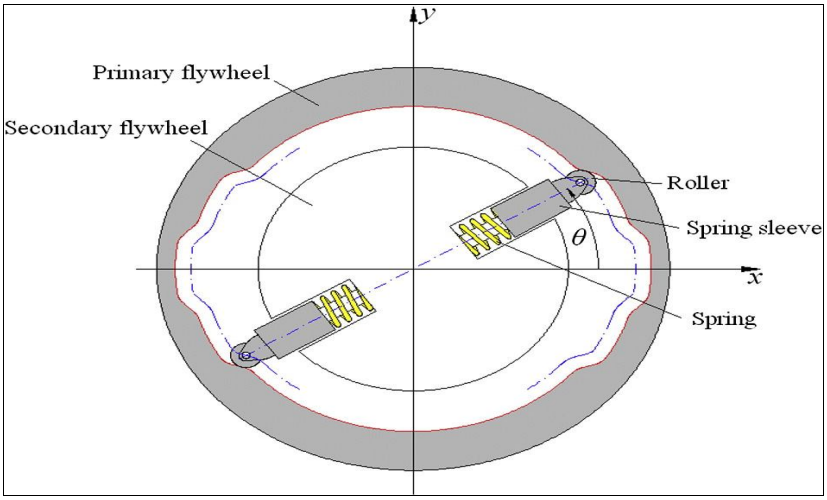

Fig. 6. Schematic diagram of the componants

This DMF adopts two sets of compensation devices, which are mounted on the secondary flywheel, as presented in Fig. 5. The compensation devices consist of a roller, spring sleeve and spring, among which the two compensation devices can slide in the chute of the secondary flywheel. The profile line of the inner wall of the primary flywheel is shaped to produce a counter torque through the mentioned compensation devices. As shown in Fig. 5, when the torsional angle θ increases in an anticlockwise direction to the compensation positions (i.e., segment 1–2 or 3–4), the length of the spring in compensation devices will decrease in its radial direction. Thus, a force will appear on the inner wall of the primary flywheel to produce a compensation torque. On the contrary, when θ increases in a clockwise direction to the compensation positions, the compensation devices will also produce a
compensation torque in the opposite direction.

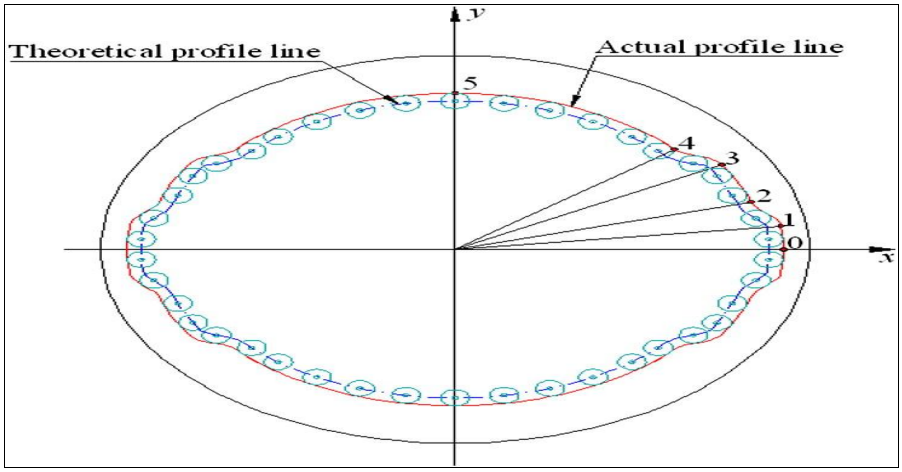

Fig 7: Compensation profile line.

In Fig. 7, the dotted line indicates the theoretical profile line, which is the track of the roller center. A series of roller circles are drawn with the roller radius and center at the points on the theoretical profile line. In this case, the envelop line of these circles is the actual profile line (i.e., the inner profile line of the primary flywheel). Segments 0–1, 2–3 and 4–5 are circular arcs, and segments 1–2 and 3–4 indicate the compensation profile lines. The left upper quadrant is the mirror image of the right upper quadrant by taking the y axis as the symmetry axis, and the left lower quadrant and the right lower quadrant are the mirror images of the left upper quadrant and the right upper quadrant by taking the x axis as the symmetry axis.

5. Theoretical calculation and Experiment

5.1. Theoretical calculation: A 2.0 L engine carrying this new DMF is studied in this paper. The main parameters of the DMF are as follows: Main stiffness Kθ1 = 4.0 N·m/°, whose acting range is 0° ≤ θ b 12°; Kθ2 = 10.0 N·m/°, whose acting range is 12° ≤ θ b 35°; Kθ3 = 24.0 N·m/°, whose acting range is 35° ≤ θ b 40°. The start angle of compensation segment AB is θa = 7°, and its end angle θb = 17°; the start angle of compensation segment CD is θc = 31°, and its end angle θd = 40°, as presented in Fig. 9. The maximum radius of the compensation profile line is R1 = 133 mm, and the stiffness of the spring in compensation device is Kb = 12.0 N/mm.

Following coefficients can be achieved: a0 = 14.70, a1 = − 0.20, a2 = 0.30, a3 = 0.0, b0 = 1496.7106, b1 = − 109.6626, b2 = 2.8231, and b3 = − 0.0192. From Eqs. (20) to (22), R2 = 126.97 mm, and R3 = 122.87 mm are obtained. The radius of the roller is taken r = 7 mm. Based on the above parameters, the theoretical and actual profile lines for the right upper quadrant are obtained as shown in figure 8.

5.2. Experiment: Torque characteristic experiments are carried out on a CTT1000 microcomputer control electronic torsion testing machine with a maximum test capacity of 1000 N·m at the Mechanical Experiment Center of Chongqing University, as shown in Fig. 11a. The secondary flywheel is jointed to the engine base, while the primary flywheel to power driving head. Meanwhile, test data is communicated to a computer via USB at rate of 12 Mb/s by bulk mode. In the experiment, the step of the torsion angle and the maximum value of the torsional angle are set as 0.1°/s and 40° respectively. The whole test process is controlled at a constant speed by the microcomputer, which can display the current, the torque, torsional angle and other experimental data. The test will stop automatically when the torsional angle reaches the setting data. Fig. 11b shows the picture of the torque test curve on the computer screen at the torsional angle of 40°.

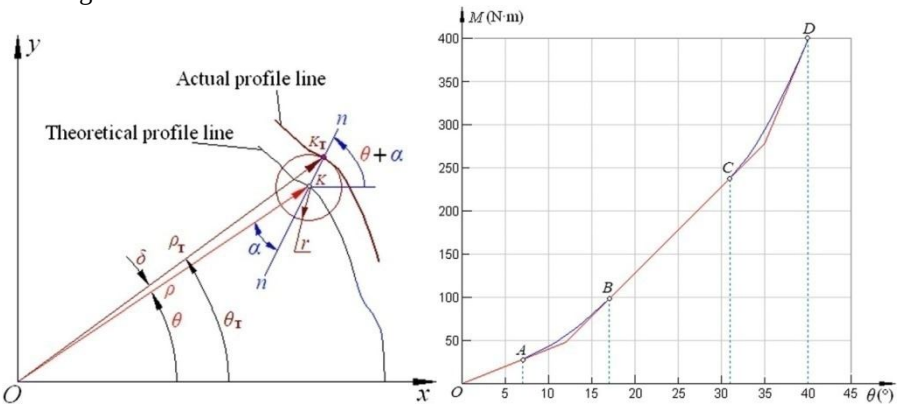

Fig 8: Torque Characteristics actual vs Theoretical profile

The comparison between theoretical and experimental torque characteristics curves is exhibited in Fig. 12. It shows that the theoretical torque as well as the experimental torque increases continuously with increasing torsional angle θ, and the experimental result is closely in accordance with the theoretical result. The corresponding data are listed in Table 1.

6. Dynamic characteristics of DMF

6.1. Torsional stiffness characteristics

Through the derivation of the torque expressed by Eq. (9): $KL = dML(\theta)/d\theta$, the theoretical stiffness curve is obtained. Suppose that the torque data obtained through test is expressed as $MS(\theta)$. By using least square fitting and the derivation of this fitting curve: $K\theta S = dMS(\theta)/d\theta$, the test stiffness is also obtained. Fig. 13 presents the theoretical and experimental stiffness characteristics. It can be seen that the two kinds of the stiffness are close to each other. Moreover, the changes of stiffness are continuous, which can avoid the impact caused by the abrupt changes of stiffness and reduce the vibration of the power transmission system.

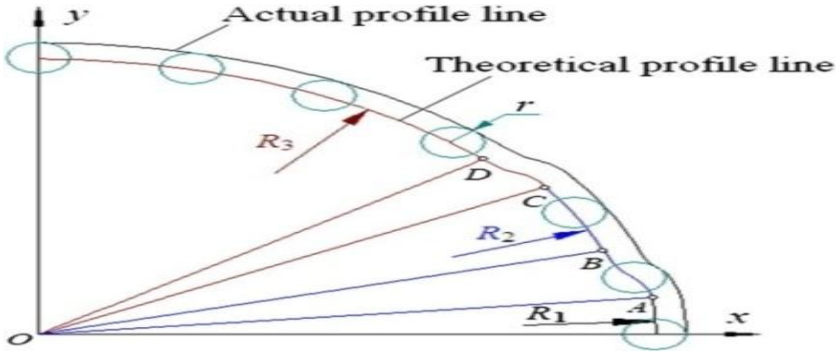

Fig 9: Torsion Stiffness actual vs Theoretical profile

6.3. Realization of eliminating inertia force

Although the mass of the compensation device is small, it will produce a great inertia force when the flywheel operates at a high speed. An inertia balance mechanism, as shown in Fig. 10, is 8. developed, with which the inertia force can be balanced. In the compensation device, the guide sleeve with a dovetail structure is embedded by interference fit into the dovetail groove of the secondary flywheel. To reduce the weight of the moving parts of the compensation device, a needle bearing without an inner ring (i.e., the roller in Fig. 10) and a spring sleeve with high strength aluminum alloy are employed. Besides this, the bottom of the compensation spring is linked with the secondary flywheel to prevent the spring from moving along with the spring sleeve. For the inertia balance mechanism, the bary-center of the swing link is located on its oscillating center, and the counterbalance is used to balance the inertia force of the moving parts of the compensation device. A needle roller bearing without inner ring is also employed in the arc chute of the secondary flywheel, and outer ring of the bearing is put into the arc groove. The integration of the compensation device and inertia balance mechanism has simple structure and can be easily assembled.

Fig 10: Actual Setup of testing

Table 1: Data of the theoretical and actually measured torque.

		-δa		θ	ML	MS	δ
(°	(N ·	(N ·	(%)	(°	(N ·	(N ·	(%)
1	4.00	5.42	35	2	138	140	2.0
2	8.00	9.03	12	2	148	149	1.2
3	12.00	12.64	5.3	2	158	160	1.7
4	16.00	16.25	1.5	2	168	170	1.5
5	20.00	20.77	3.8	2	178	181	1.9
6	24.00	24.38	1.5	2	188	190	1.3
7	28.00	27.99	0.3	2	198	200	1.2
8	32.00	32.51	1.5	2	208	211	1.5

9	37.20	37.02	0.4	2	218	221	1.4
10	42.70	43.34	1.5	3	228	231	1.3
11	48.80	48.76	0.0	3	238	242	2.0
12	55.50	55.98	0.8	3	249	254	2.2
13	62.80	64.11	2.0	3	261	269	2.7
14	70.70	72.24	2.1	3	276	281	1.7
15	79.20	80.36	1.4	3	293	298	1.8
16	88.30	90.29	2.2	3	311	317	0.2
17	98.00	100.2	2.2	3	331	336	1.6
18	108.0	110.1	2.0	3	352	358	1.7
19	118.0	120.0	1.7	3	374	380	1.5
20	128.0	130.0	1.7	4	400.	403.	0.7

According to the actual vehicle model, $K_{\theta B} = 574$ N·m/°, the variations of n_1 and n_2 with $K_{\theta A}$ can be obtained, as listed in Table 1. When $K_{\theta A}$ N 16 N·m/°, the first-order resonance speed n_1 of the engine is higher than its idle speed. However, the rotational speed of engine, which is at a large torsional angle with high torque, is much higher than the idle speed. Thus, the first-order resonance vibration will not occur.

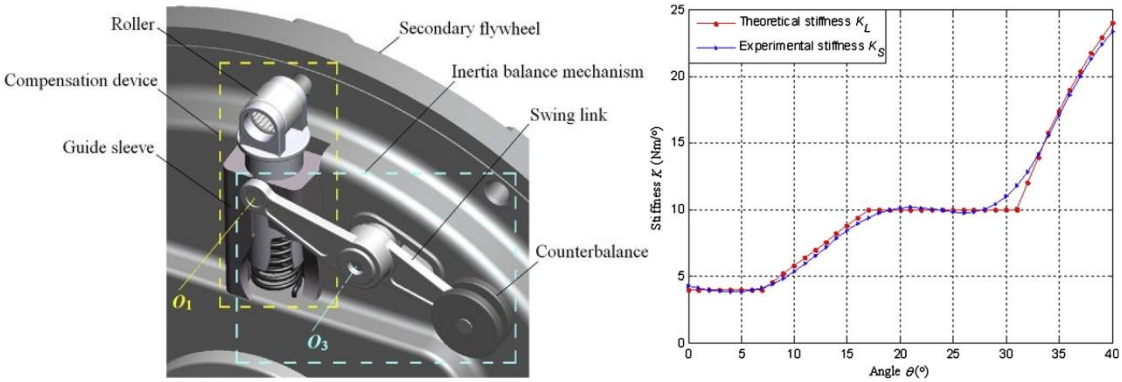

Fig 11: Proposed design

The torsional stiffness KθA of the DMF at small torsional angle can be designed to be lower, in the present study, KθA = 4 N·m/°. The aim of this dealing is to reduce the first-order resonance speed, and further to make the engine able to operate at a lower idle speed so as to reduce energy consumption. Meanwhile, there exists a high counter torque at large torsional angles, in which case DMF can be well suited for powerful engines.

7. Conclusion

By adding a compensation device, a new DMF with continuously variable stiffness is presented to release the impact produced by the step changes of stiffness. The numerical and experimental results prove that the proposed design theory of the DMF based on compensation principle can realize the characteristics of non-linear high counter torque and continuously variable stiffness, and meet the requirements of small stiffness at small torsional angle conditions and high counter torque and large stiffness at large torsional angle. Compared with traditional multi-piece step stiffness DMF, this new DMF can avoid impact and noise more effectively. The proposed inertia balance mechanism with a simple structure is proposed to eliminate the inertia force effect on the primary flywheel produced by the moving parts of the compensation device, which can accurately put the theoretical compensation torque into practice.

References

[1]. M. Zink, M. Hausner, LuK clutch systems and torsional dampers, Schaeffler Symposium, 2010, pp. 827.
[2]. Fidlin, R. Seebacher, DMF Simulation Techniques, 8th LuK symposium, 2006, pp. 55–71.
[3]. Walter, U. Kiencke, S. Jones, T. Winkler, Anti-jerk & idle speed control with integrated sub-harmonic vibration compensation for vehicles with dual mass flywheels, SAE Int. J. Fuels Lubr. 1 (1) (2009) 1267–1276.
[4]. Filipović, D. Bibić, A. Milašinović, A. Blažević, A. Pecar, Preliminary selection of basic parameters of different torsional vibration dampers intended for use in medium-speed diesel engines, Trans. FAMENA 36 (3) (2012) 79–88.
[5]. N. Cavina, G. Serra, Analysis of a dual mass flywheel system for engine control applications, SAE Trans. 113 (7) (2004) 280–286.
[6]. T.S. Kang, S.K. Kauh, K.P. Ha, Development of the displacement measuring system for a dual mass flywheel in a vehicle, Proc. Inst. Mech. Eng. Part D J. Automob. Eng. 223 (10) (2009) 1273–1281.

[7]. S. Sangue, G. Lepoint, T. Le Bournault, New approach to measure instantaneous angular behavior of a dual mass flywheel, Seoul 2000 World Automotive Congress, Seoul, Korea, 2000, pp. 12–15.
[8]. A. Balluchi, L. Benvenuti, C. Lemma, P. Murrieri, A.L. Sangiovanni-Vincentelli, Hybrid Models of an Automotive Driveline, Tech. rep., Parades, 2004.
[9]. S. Theodossiades, M. Gnanakumarr, H. Rahnejat, P. Kelly, Effect of a dual-mass flywheel on the impact-induced noise in vehicular powertrain systems, Proc. Inst. Mech. Eng. Part D J. Automob. Eng. 220 (6) (2006) 747–761.
[10]. U. Schaper, O. Sawodny, T. Mahl, U. Blessing, Modeling and torque estimation of an automotive dual mass flywheel, American Control Conference, 2009. ACC'09. IEEE, 2009, pp. 1207–1212.

AUTHOR

Mr. Lamkane Anup Abasaheb has complited his bachors education in engineering in Mechanical Engg. From R.E.P. Bhlki, Karnataka State. Currently working is senior Lecturre in B.M. Polytechnic, Belati , Solapur since from last 4 years. Also he is completing his Masters in Mechanical Engineering (design Stream).